Philosophical Magazine,
Vol. 87, No. 10, 1 April 2007, 1513–1529

Taylor & Francis
Taylor & Francis Group

Dislocation transmission across the Cu/Ni interface: a hybrid atomistic–continuum study

M. A. SHEHADEH*†, G. LU†, S. BANERJEE‡, N. KIOUSSIS† and N. GHONIEM§

†Department of Physics and Astronomy, California State University, Northridge, CA 91330-8268, USA
‡Engineering Technology Department, Saint Louis University, Saint Louis, MO 63103, USA
§Department of Mechanical and Aerospace Engineering, University of California, Los Angeles, CA 90095, USA

(*Received 12 July 2006; in final form 6 October 2006*)

The strengthening mechanisms in bimetallic Cu/Ni thin layers are investigated using a hybrid approach that links the parametric dislocation dynamics method with *ab initio* calculations. The hybrid approach is an extension of the Peierls–Nabarro (PN) model to bimaterials, where the dislocation spreading over the interface is explicitly accounted for. The model takes into account all three components of atomic displacements of the dislocation and utilizes the entire generalized stacking fault energy surface (GSFS) to capture the essential features of dislocation core structure. Both coherent and incoherent interfaces are considered and the lattice resistance of dislocation motion is estimated through the *ab initio*-determined GSFS. The effects of the mismatch in the elastic properties, GSFS and lattice parameters on the spreading of the dislocation onto the interface and the transmission across the interface are studied in detail. The hybrid model shows that the dislocation dissociates into partials in both Cu and Ni, and the dislocation core is squeezed near the interface facilitating the spreading process, and leaving an interfacial ledge. The competition of dislocation spreading and transmission depends on the characteristics of the GSFS of the interface. The strength of the bimaterial can be greatly enhanced by the spreading of the glide dislocation, and also increased by the pre-existence of misfit dislocations. In contrast to other available PN models, dislocation core spreading in the two dissimilar materials and on their common interface must be simultaneously considered because of the significant effects on the transmission stress.

1. Introduction

The influence of interfaces on the mechanical properties of multiphase and polycrystalline materials is ubiquitous. The mechanical properties of an interface are determined, in large part, by the nature of the chemical bonding at the interface, which may be significantly different from that within either of the materials meeting

*Corresponding author. Email: mutasem@csun.edu.

Philosophical Magazine
ISSN 1478–6435 print/ISSN 1478–6443 online © 2007 Taylor & Francis
http://www.tandf.co.uk/journals
DOI: 10.1080/14786430601055379

at the interface. The variation of the generalized stacking fault energy surface (GSFS) of the interface, the existence of misfit dislocations and the lattice mismatch can act as barriers to dislocation motion and transmission across the interface. In recent years, there has been considerable interest in the mechanical and structural properties and the deformation mechanisms of metallic multilayer systems, which display remarkably high mechanical strength and hardness comparable to their theoretical strength [1]. It has been found experimentally that the hardness and ultimate tensile strength of nano-layered structures increases with decreasing bilayer thickness, in a relation analogous to the Hall–Petch behaviour to some critical layer thickness. At smaller wavelengths, the hardness is seen to increase more rapidly, with Hall–Petch exponents of the order of unity or greater, to some peak stress value that is much greater than that attainable by traditional microstructures. Thus, multilayers composed of alternating layers made of metals such as Cu, Ni, Cr and Nb exhibit peak strengths on the order of few GPa at layer thickness of few nanometres [2, 3], compared to the yield strength values of few tens of MPa in bulk Cu, Ni, Cr and Nb.

The dramatic enhancement of multilayer strength has been generally attributed to the following factors: the mismatch in the elastic properties which results in image forces on the dislocation; the mismatch in the GSFS between incoming and outgoing planes which plays a major role in determining the core properties of the dislocation; the mismatch in the lattice parameters that leads to the generation of coherency stress across the interface; and the GSFS of the interface which may suppress or enhance the spreading of the dislocation core from the glide plane to the interface. Additionally, the existence of misfit dislocations affects the overall strength of multilayers as a result of their mutual interaction with glide dislocations.

A pronounced size effect has been observed in thin multilayers systems as different deformation mechanisms operate at different length scales. Whereas the behaviour of multilayers can be described by a scaling law in the submicron length scale, deviation from this scaling law occurs at the nanoscale and the effect of discrete or even single dislocation strengthening mechanism applies [4]. At the nanoscale, the strengthening mechanisms fall into several broad categories. The first mechanism is the classic Hall–Petch model of dislocation pileups [5–7]. The second mechanism was introduced by Koehler [8], where the image forces imposed by the layers of alternating materials restrict the motion of dislocations [9]. The dislocations are attracted towards (repelled from) the interface by the decrease (increase) in line energy as a dislocation moves toward the material with lower (higher) elastic constants. Another deformation mechanism involves the formation and propagation of so-called ''Orowan'' bows within the layer [10].

From the point of view of theory, there have been approaches based on the continuum elasticity approach for both ''welded'' and ''slipping'' interfaces [11]. Recently, Han and Ghoniem [12] have developed a Green's function approach for the elastic field of three-dimensional dislocation loops in anisotropic multilayer materials. As expected, the image force, which is accurately described by linear elasticity [13, 14], diverges in the vicinity of the dislocation core. In order to overcome this difficulty, an arbitrary cut-off radius, r_0, is generally introduced but its actual value is highly uncertain. Consequently, important quantities, such as the

critical stress required to make the dislocation cross the interface, are not accurately determined unless r_0 is ''calibrated'' with atomistic calculations.

On the other hand, molecular dynamics (MD) simulations have been used extensively to study different deformation mechanisms in bimaterials. The MD simulations of Hoagland *et al*. [15] have shown that coherency stresses and interface dislocations play a critical role in determining how the layered microstructure behaves under an applied load. The MD simulations of Rao and Hazzledine [16] demonstrated that a screw dislocation in Cu forms interfacial dislocations in the Cu/Ni twinned interface and hence prefers to spread on the interface rather than to transmit to Ni. Other MD simulations have also indicated that the intrinsic resistance to slip transmission for Cu/Nb system can originate from the low shear strength of the interface [17]. Although MD simulations are very useful in revealing the atomistic mechanism for the strengthening effect in multilayers, they suffer from the lack of reliable empirical potentials for treating interatomic interactions across the interface [18], especially when one considers new materials for which empirical interatomic potentials are not available.

Over the past few years, the Peierls–Nabarro (PN) model combined with *ab initio*-determined GSFS has been used to study the dislocation core properties in bulk materials [18–21] and the effect of chemistry on the dislocation core properties in aluminium [22]. The GSFS represents the two-dimensional energy profile when the two crystal halves above and below the glide plane are shifted rigidly against each other by a constant disregistry vector, **u**. The GSFS-based approach is essentially a local formulation of the PN model and it assumes slowly varying slip distributions. For a dislocation with a wide core as in the case of Cu and Ni, the strain gradient is relatively small, and therefore, the local formulation should give a reasonable description of the dislocation core structure. Although a non-local formulation of the PN model has been proposed [23], it has not been widely used due to its complexity.

Anderson *et al*. [24–26] have extended the PN model to investigate the transmission of a screw dislocation across a coherent, slipping bimaterial interface. Anderson and Li [24] and Shen and Anderson [26] developed a 2D PN model for the transmission of a screw dislocation across a slipping and welded interfaces. Their models were able to predict several trends that give more insight to understanding the strengthening mechanisms in bimetallic materials. A general observation made is that slipping interfaces delocalize and trap the core of an incoming dislocation. Anderson's model is limited in two respects: (i) rather than using an *ab initio* description of the atomistic shear on both the glide and interface planes, it employs a simple sinusoidal form of the γ surface which in turn does not allow dissociation, and (ii) the possibility of a pure screw dislocation to dissociate with a Burgers vector containing an edge component is neglected. The present model is similar to that of Anderson and Li, and makes use of *ab initio* and parametric dislocation dynamics (PDD) [27] computations to resolve these two issues.

We have developed an extension of the PN model which integrates the atomistic nature from *ab initio* electronic structure calculations into the PDD method [28]. The GSFS provides a *two-dimensional representation* of the stacking fault energy at zero temperature. Both coherent and incoherent interfaces are considered and the

lattice resistance of dislocation motion is captured through the *ab initio*-determined GSFS. In this study, the core properties of a pure screw dislocation as it moves from Cu to Ni are investigated. The effects of the GSFS of the interface on dislocation core spreading and on the transmission stress is also determined. Additionally, the effect of pre-existing misfit dislocation on interfacial strength and dislocation core spreading is investigated.

2. PN model for the Cu/Ni interface

The PN model used in this work is an extension to the parametric dislocation dynamics model for bulk materials developed by Banerjee *et al.* [28]. In this approach, the full dislocation is represented by a set of N fractional Volterra dislocations with fractional Burgers vector $db = b/N$. A right handed coordinate system as shown in figure 1a is used. The dislocation line is chosen to be along the z direction. In the case of a pure screw dislocation a sufficient amount of edge components is added by introducing $N/2$ positive and $N/2$ negative fractional edges (see figure 1b). In contrast to the treatment of Anderson, the atomic displacements of the dislocation have components in all three directions rather than only along the direction of the Burgers vector. The displacement components of the slip u_x and u_z are determined from the positions of the fractional dislocations of edge and screw types with fractional Burgers vector. The equilibrium structure of the dislocation core is obtained by seeking the equilibrium configuration of these fractional dislocations. Physically, this corresponds to balancing the elastic force and the lattice restoring force for each infinitesimal dislocation across the glide plane. For a mixed dislocation with components (b_e, b_s) the displacement components can be approximated as

$$u^e(x) = u_x = \sum_{i=1}^{N} b_e^i \tan^{-1}(x - x_i) + \frac{b_e}{2} \tag{1}$$

$$u^s(x) = u_z = \sum_{i'=1}^{N} b_s^{i'} \tan^{-1}(x - x_{i'}) + \frac{b_s}{2} \tag{2}$$

where $b_e^i = (b_e/N)$, $b_s^{i'} = (b_s/N)$ are the Burgers vectors of the fractional dislocations, N is the total number of dislocations of edge and screw type, and x_i, $x_{i'}$ are the corresponding positions. The net elastic force resulting from the interaction between these fractional dislocations is balanced against the lattice restoring force derived from the GSFS across the glide plane. In this formulation, the GSFS of Cu, Ni, and the Cu/Ni interface are calculated using first-principles *ab initio* method.

The PN model has been modified to investigate the strengthening mechanisms in slipping and rigid Cu/Ni bimaterials. The effects of the mismatch in the elastic properties, the mismatch in the GSFS, the mismatch in the lattice parameters and the existence of misfit dislocations are explicitly taken into account.

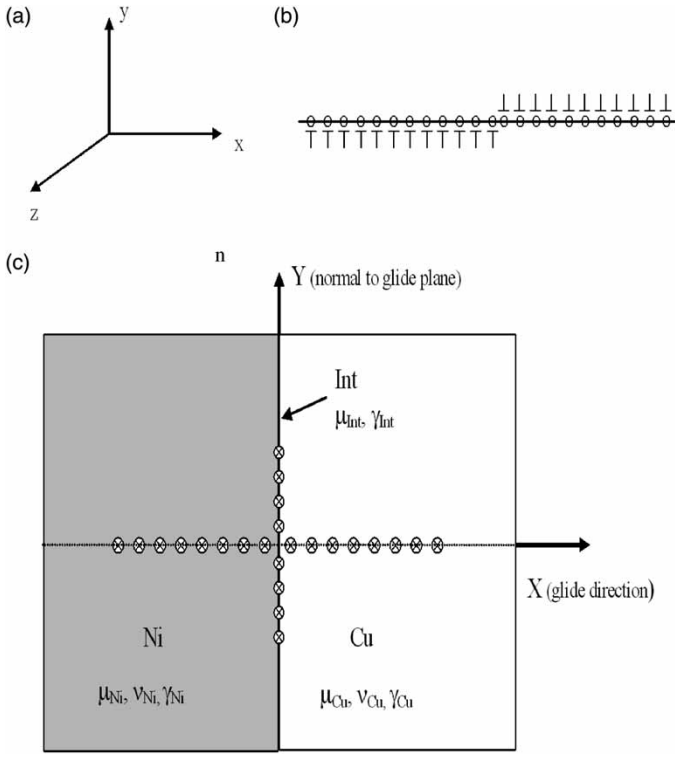

Figure 1. (a) The Cartesian coordinate system used in the simulations; (b) schematic showing the idea of adding extra positive and negative edge components for pure screw dislocations; (c) schematic of the discretized Peierls screw dislocation during the transmission process from Cu to Ni. The Burgers vector and the line sense of the dislocation are along the z direction. The fractional Burgers vector in Cu is b_{Cu}/N, in Ni is b_{Ni}/N and on the interface $b_{\mathrm{Ni}}/2N + (b_{\mathrm{Cu}} - b_{\mathrm{Ni}})/2N$.

For a slipping interface, part of the dislocation content can be accommodated by the interface through dislocation core spreading. Any dislocation that moves from the glide plane to the interface is divided into two identical fractional dislocations, symmetrically placed with respect to the slip plane. In particular, the mismatch in lattice constant between Cu and Ni is accommodated by the fractional residual slip on the interface. The continuity of the Burgers vector requires that:

$$b_{Cu} = n_{Cu} db_{Cu} + n_{Ni} db_{Ni} + 2n_{Int} db_{Int}, \tag{3}$$

where $N = n_{Cu} + n_{Int} + n_{Ni}$, n_{Cu}, n_{Ni}, n_{Int} are the number of fractional dislocations in Cu, Ni, and interface, respectively, and $db_{Cu} = b_{Cu}/N$, $db_{Ni} = b_{Ni}/N$, and $db_{Inti} = b_{Cu}/2N$.

For the Cu/Ni bimaterial problem, the equilibrium condition of a fractional dislocation i depends on whether the fractional dislocation is in Cu, Ni or

on the interface. The total force on a fractional *screw* dislocation i can be expressed as:

$$F^{T_s}_{i_{Cu}} = \left[\sigma^{ext}_s + \sum_{j=1}^{n_{Cu}} \sigma^{Cu-Cu}_s(x_i,x_j) + \sum_{j=1}^{2n_{\text{int}}} \sigma^{Cu-Int}_s(x_i,y_j) + \sum_{j=1}^{n_{Ni}} \sigma^{Cu-Ni}_s(x_i,x_j)\right] b_{i_{Cu}} + f^{s}_{i_{Cu}} + f^{Coh}_{i_{Cu}} \tag{4}$$

$$F^{T_s}_{i_{Int}} = \left[\sigma^{ext}_{Int} + \sum_{j=1}^{n_{Cu}} \sigma^{Int-Cu}_s(y_i,x_j) + \sum_{j=1}^{2n_{\text{int}}} \sigma^{Int-Int}_s(y_i,y_j) + \sum_{j=1}^{n_{Ni}} \sigma^{Int-Ni}_s(y_i,x_j)\right] b_{i_{Int}} + f^{s}_{i_{Int}} + f^{Coh}_{i_{Int}} \tag{5}$$

$$F^{T_s}_{i_{Ni}} = \left[\sigma^{ext}_s + \sum_{j=1}^{n_{Cu}} \sigma^{Ni-Cu}_s(x_i,x_j) + \sum_{j=1}^{2n_{\text{int}}} \sigma^{Ni-Int}_s(x_i,y_j) + \sum_{j=1}^{n_{Ni}} \sigma^{Ni-Ni}_s(x_i,x_j)\right] b_{i_{Ni}} + f^{s}_{i_{Ni}} + f^{Coh}_{i_{Ni}} \tag{6}$$

where x_i and y_i are the positions of the fractional dislocations on the glide and the interface planes, respectively. The first term in each equation (σ^{ext}) is the externally applied stress along the dislocation line; the second, third and fourth terms are the stress exerted on the fractional dislocation from other fractional dislocations located in Cu, on the interface, and in Ni, respectively; the fifth term is the lattice restoring force derived from the GSFS, and the last term is the coherency stress. The expressions for the stress in the above equations are normalized with respect to the average shear modulus $\bar{\mu} = (\mu_{Cu} + \mu_{Ni})/2$. Note that the fourth term in equation (4) (σ^{Cu-Ni}_s) and the second term in equation (6) (σ^{Ni-Cui}_s) represent the image stresses (Koehler stresses) resulting from the mismatch in the elastic properties between Cu and Ni. The explicit expressions of the image stress for the screw and edge components are given by Anderson and Li [24] and Head [14], respectively.

In our formulation we assume that there is no dislocation climb and therefore only screw dislocations can spread out onto the interface. Additionally, the external stress and coherency stress are applied only to the screw components on the glide plane; i.e. $\sigma^{ext}_{Int} = 0$ and $f^{Coh}_{i_{Int}} = 0$. The expression for the net force on a fractional *edge* dislocation i is similar to those for a fractional screw dislocation in equations (4) and (6), but with the following differences: no external stress is applied on the edge component and there is no stress contribution from the interface because the fractional edge dislocation is confined to the glide plane.

The edge and screw components of the lattice restoring force, obtained from the GSFS are given by

$$f^{e}_i = -b^i_e \left.\frac{\partial \gamma}{\partial u_e}\right|_{x=x_i} \tag{7}$$

$$f^{s}_i = -b^i_s \left.\frac{\partial \gamma}{\partial u_s}\right|_{x=x_i}, \tag{8}$$

where γ is the GSFS.

Table 1. Material properties of Cu and Ni used in the simulations: μ is the shear modulus; b is the Burgers vector; γ_{int} and γ_{uns} are the intrinsic and unstable stacking fault energies, respectively; and B is the drag coefficient.

Material	μ (GPa)	b (Å)	γ_{int} (mJ m^{-2})	γ_{uns} (mJ m^{-2})	B (N s m^{-1})
Ni	80	2.5	163	225	10^4
Cu	50	2.6	53	350	10^4

The force due to the coherency stress results from the mismatch in the Cu/Ni lattice parameters. The calculated *uniaxial* coherency stress in Cu/Ni bimaterial is around 2.5 GPa [29], which is equivalent to 1.0 GPa when resolved on the glide plane. In this work the coherency stress is assumed to be of a step function centered at the interface with the value $\sigma_i^{Coh} = \pm 1.0$ GPa. The plus (minus) sign indicates compressive (tensile) stress in Cu (Ni).

It is worth mentioning that the geometry used in the current work assumes that the interfacial (100) plane is perpendicular to the glide plane (111) to avoid additional computational complexities. However, in reality the glide plane is inclined with respect to the interfacial plane by an angle $\theta = 54.5^\circ$, which in turn leads to asymmetric dislocation core spreading due to the modification of the image forces.

In this quasistatic framework, the dislocation glide is controlled by drag, and hence the dislocation velocity is proportional to the resolved shear stress. Having determined all the force components, the equilibrium position of each fractional dislocation is computed according to the drag dislocation dynamics relation,

$$F_i^T = B\frac{dx_i}{dt}, \tag{9}$$

where B is a drag coefficient to update the position x_i of the dislocation at each time step until the system reaches equilibrium (see table 1).

The interfacial strength is determined by computing the critical value of the external stress required to transmit the dislocation from Cu to Ni. The external stress is applied incrementally to push all fractional dislocations across the interface. When the leading dislocation reaches a critical distance of $0.04b_{\text{Cu}}$ from the interface, two pathways can be taken by the dislocation: it can either spread onto the interface or continue gliding on the original slip plane into Ni. The pathway with a lower energy will be taken by the dislocation. The process is repeated for all fractional dislocations while the applied stress keeps increasing until it reaches a critical value that allows dislocation transmission. This critical value is defined as the transmission stress τ_{critical}.

3. Results and discussion

3.1. *Generalized stacking fault energy surface*

The Cu/Ni bimaterial system is modelled as two semi-infinite homogenous and isotropic regions connected at the interface, as shown in figure 1c. The glide planes of

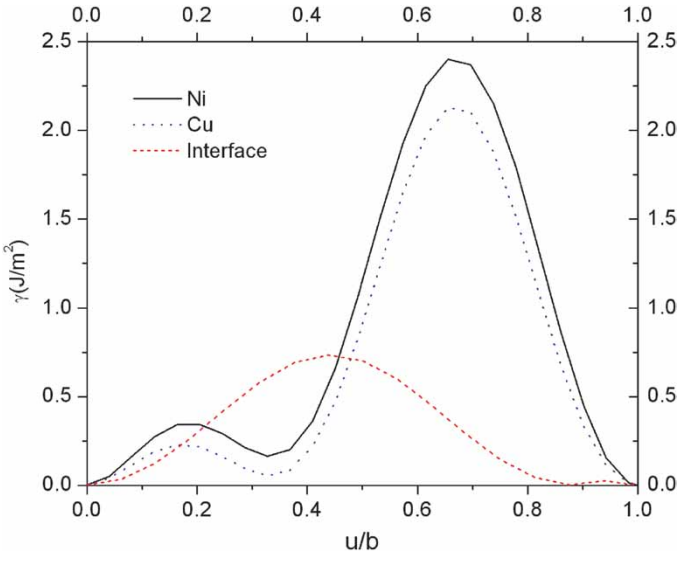

Figure 2. *Ab initio* stacking fault energies for Ni and Cu along the [112] direction and for the interface along [100] direction.

Cu and Ni are assumed to be coplanar and normal to the interface. A pure screw dislocation of Burgers vector 1/2 [110] is placed in Cu (soft material) gliding in (111) plane. The electronic structure calculations of the GSFS were done using the projector augmented-wave (PAW) method [30] as implemented in the VASP code [31, 32]. The *ab initio*-determined GSFS projected along the [121] direction for the pure Cu and Ni and along the [001] direction for the Cu/Ni interface are shown in figure 2. The first energy maximum encountered along the [121] direction for the Cu and Ni is the unstable stacking fault energy (γ_{uns}) which represents the lowest energy barrier to nucleate a dislocation from a crack tip. The first energy maximum encountered along the [121] direction for the Cu and Ni is the unstable stacking fault energy which represents the lowest energy barrier to nucleate a dislocation from a crack tip at 0 K. At finite temperatures, the effective energy barrier for dislocation nucleation will be reduced by both thermal excitations and the fact that dislocation nucleus may take a three-dimensional shape. The local minimum on the other hand, corresponds to the intrinsic stacking fault energies (γ_{intrin}). The calculated values of γ_{uns} are 225 mJ m^{-2} and 350 mJ m^{-2} for Cu and Ni, respectively, whereas the values of γ_{intrin} for Cu and Ni are 53 mJ m^{-2} and 163 mJ m^{-2}, respectively. These values are in good agreement with other calculations [33]. As expected, the GSFS of the interface is symmetric along the [110] direction and it has unstable stacking fault energy of 730 mJ m^{-2}, which is much higher than the corresponding value of Ni and Cu. The absence of a saddle point in the GSFS of the interfaces suggests that the full dislocation on the interface does not dissociate. The shear modulus, Burgers vectors and the energy values for the various stacking fault energies for Ni and Cu are listed in table 1.

3.2. *Displacement and density profiles*

The large increase in the mechanical strength of nano-layered materials is widely attributed to the presence of interfaces. Several factors can affect the mechanical and physical properties of the interface such as: the unstable stacking fault energy of the interface, γ_{int}, which is a measure of the propensity of interfacial sliding and which is directly related to the electron charge bonding across the interface, the presence of misfit dislocations, and the presence of impurities. The smaller γ_{int} is the easier it is for the interface to slide, thus allowing the dislocation to spread onto the interface.

Figure 3 shows the equilibrium edge and screw displacement and the corresponding Burgers vector density $\rho(x)$ of the dislocation for three values of applied stress. The edge and screw Burgers vector density are defined by $\rho_e(x) = du_e/dx$, and $\rho_s(x) = du_s/dx$. The screw dislocation, originally placed in the soft material ($x > 0$) is pushed towards the Cu/Ni interface. For relatively low values of applied stress (around 2.0 GPa), the dislocation core in Cu dissociates into two partials bounding a stacking fault with a separation distance of about $7b$ (figure 3a). As the external stress increases, the dislocation approaches the interface but remains dissociated. However; the dislocation core structure has changed significantly. First, the dislocation Burgers vector density accumulates on the leading partial at the expense of the trailing partial (figures 3b and 3c). Second, the dislocation core constricts steadily and the two partials become significantly overlapped (figure 3c). Note, that the maximum value of the screw component of the displacement in Cu is 2.35 Å, whereas the Burgers vector of Cu is 2.6 Å. This reduction of Burgers vector is a result of the energetically favourable spreading of the core onto the interface. Our results suggest that the dislocation spreading process proceeds via the following mechanism: when the leading fractional dislocation reaches the vicinity of the interface it spreads on it, if it is energetically favourable. As the external stress is increased, the trailing fractional dislocations follow and spread onto the interface. The spreading process continues until the interface can no longer accommodate additional slip. At the critical value of the applied stress, once the leading dislocation on the glide plane overcomes the interfacial barrier and is transmitted to the Ni crystal, the remaining fractional dislocations follow.

In figure 4 we show the time evolution of the displacement $u(x)$ and the Burgers vector density profiles $\rho_s(x)$ and $\rho_e(x)$ of the dislocation when the applied stress has reached its critical value of 3.35 GPa. At the initial stage of the dislocation transmission process, most of the fractional dislocations are localized in the vicinity of the interface in the Cu host (figure 4a). As the fractional dislocations relax, they get transmitted through the interface towards the Ni host till all of them pass. Note that after the dislocation gets transmitted, the density profile shows the formation of two partials with a separation distance of about $6b$ (figure 4c). The peak in the density profile at $x = 0$ indicates the formation of a ledge on the interface, in agreement with MD simulations for edge or mixed dislocations for the Cu/Ni interface [16].

3.3. *Effect of unstable stacking fault of the interface*

Interfaces can be coherent, semi-coherent or fully non-coherent. In the case of fully non-coherent structures, dislocation motion is restricted to individual layer [9],

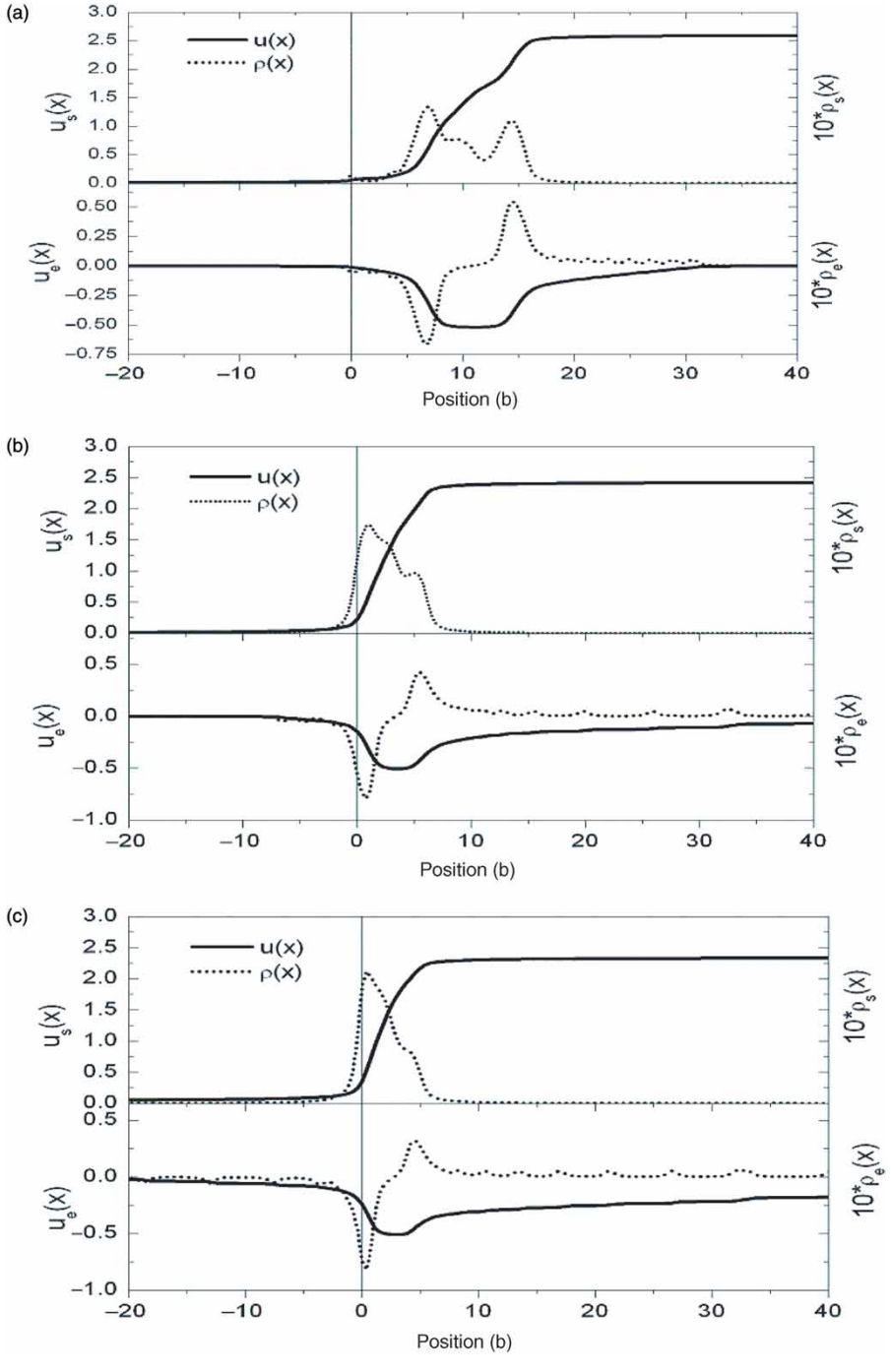

Figure 3. The displacement $u(x)$ and density $\rho(x)$ profiles for the dislocation as it moves from Cu towards Ni. The GSFS of the interface is equal to the *ab initio* value ($\gamma_{\text{int}} = \gamma_{\text{int}}^{ab}$). The profiles show the equilibrium positions of the dislocation at (a) 2.0 GPa, (b) 2.8 GPa and (c) 3.30 GPa. The continuous lines represent the screw or the edge displacements and the dotted lines represent the corresponding densities.

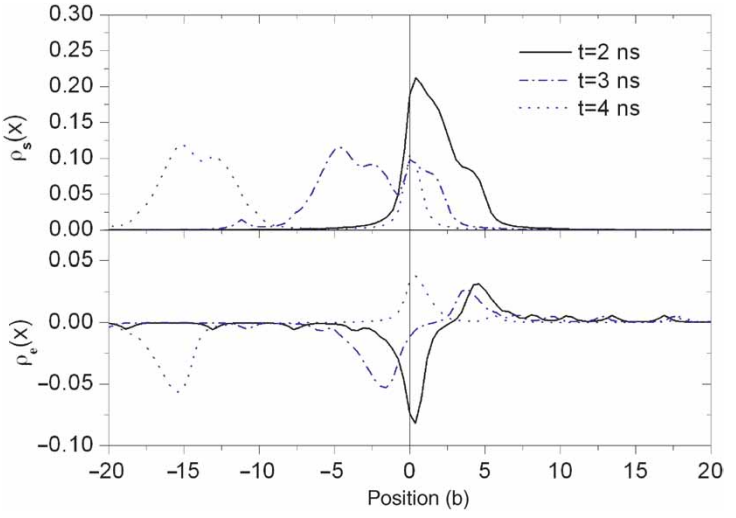

Figure 4. The dynamic evolution of the dislocation during the transmission process. The critical stress for penetration is 3.35 GPa and as the simulation time passes, the dislocation penetrates to Ni.

i.e. the interface acts as a dislocation sink. For a semi-coherent interface, as in the case of Cu/Ni, dislocation transmission across the interface is possible depending on the stacking fault energy of the interface. In order to explore the effect of interfacial sliding on the critical stress required for dislocation transmission, we have varied the value of γ_{int} with respect to its *ab initio* value $\gamma_{\text{int}}^{ab} = 730\,\text{mJ m}^{-2}$.

Figure 5 displays the dislocation displacement profiles for the screw component on the glide plane, $u_s(x)$, and on the interface plane, $u_s(y)$, for different values of the ratio, $\gamma_{\text{int}}/\gamma_{\text{int}}^{ab}$, of 1.2 (hard interface), 1.0 and 0.8 (soft interface). In each panel we show also the results for the displacement profiles for various applied stress values. As expected, as the interfacial energy barrier for sliding is reduced and the interface becomes less bonded, the percentage of the dislocation spreading on the interface increases from about 13% for $\gamma_{\text{int}} = 1.2\gamma_{\text{int}}^{ab}$ to 30% for $\gamma_{\text{int}} = 0.8\gamma_{\text{int}}^{ab}$. The spreading of fractional dislocations on the interface imposes an extra energy barrier on the transmission of the glide dislocations. The extra barrier is due to the repulsive elastic interactions between the glide and interfacial fractional dislocations and the formation of the interfacial ledge which hinders the transmission process from Cu to Ni. Consequently, the critical value of applied stress for dislocation transmission increases (decreases) to the value of 4.2 GPa (3.2 GPa) as the interfacial GSFS decreases (increases) compared to its corresponding *ab initio* value. The ledge formation is partially due to the accommodation of the mismatch in Burgers vector between Cu and Ni which is about 0.10 Å. A closer examination of figure 5b, however, shows that the screw displacement profile as the dislocation transmits from Cu to Ni has a step at the interface whose height is 0.25 Å, which is larger than the lattice constant mismatch of 0.1 Å.

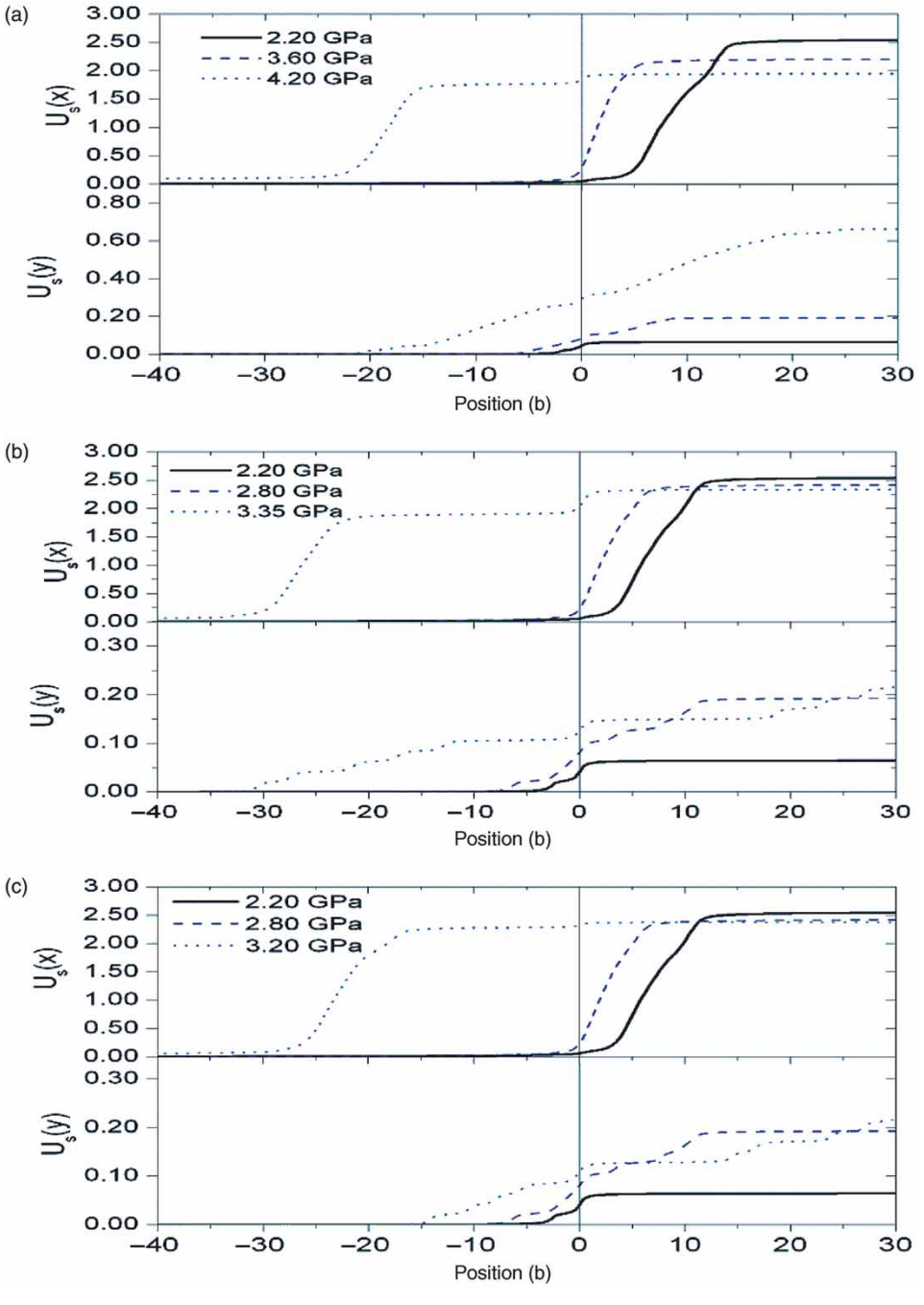

Figure 5. Snapshots of the displacement and the density profiles along the glide plane, $u_s(x)$ and $\rho_s(x)$, and along the interface plane, $u_s(y)$, for different values of the GSFS of the interface (a) $\gamma_{int} = 0.8\gamma_{int}^{ab}$, (b) $\gamma_{int} = \gamma_{int}^{ab}$ and (c)$\gamma_{int} = 1.2\gamma_{int}^{ab}$.

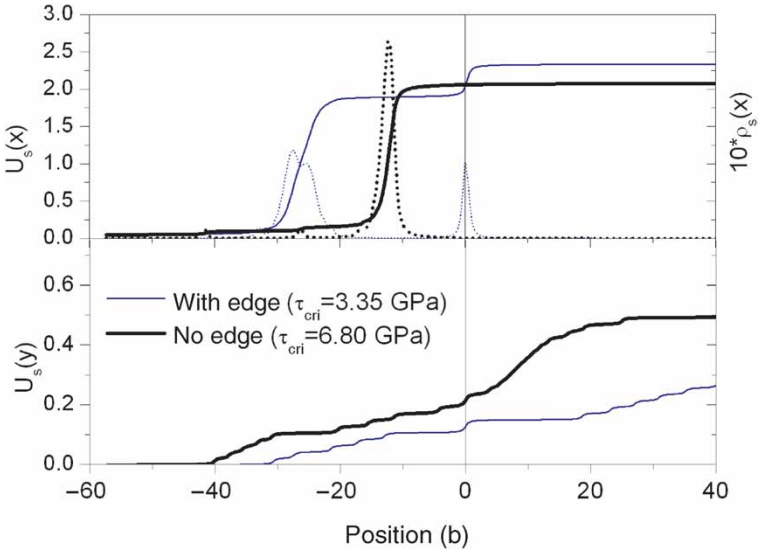

Figure 6. The displacement and the density profiles along the glide plane, $u_s(x)$ and $\rho_s(x)$, and along the interface plane, $u_s(y)$, for a pure screw dislocation, with and without the associated edge component.

3.4. *Effect of dislocation splitting*

Previous PN-based simulations [24–26] did not take into consideration the development of the edge component of a pure screw dislocation upon dissociation. This possibility results in dislocation splitting into a partial with mixed Burgers vectors, with an overall reduction of the energy, as compared to dissociation along screw components alone, which renders the dislocation with higher misfit energy. In order to explore the effect of the dislocation splitting on the spreading process, we have carried out several simulations in which we disallow the dislocation to split by considering the screw displacement only (i.e. removing the edge component associated with each screw dislocation). The results are then compared with our previous results in figures 3–5, where the edge component was taken into account explicitly.

Figure 6 shows the screw displacement and density profiles on the glide plane, $u_s(x)$ and $\rho_s\ddot{y}\,x)$, and on the interface plane, $u_s(y)$, with and without the edge components. The removal of the edge components changes the dislocation core structure considerably. First, the dislocation core does not dissociate. Second, the dislocation core becomes much narrower as reflected on the dramatic increase in the magnitude of the Burgers vector density. Finally, more dislocation core spreading onto the interface takes place which in turns leads to a significant increase in the transmission stress. By removing the edge components, the critical stress is doubled compared to the case where the edge component is taken into account explicitly. The results suggest that a constricted dislocation core can spread onto the interface much easier, which is analogous to the cross slip mechanism [21].

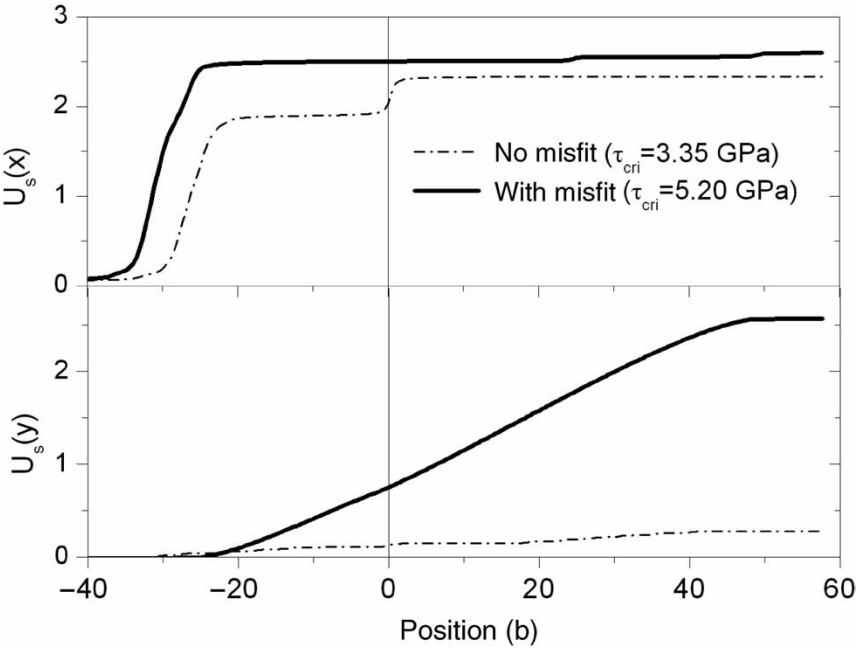

Figure 7. Effect of pre-existing misfit dislocation on the displacement and the density profiles for a screw dislocation. The displacement and density profiles "after dislocation transmission" are shown on the glide plane, $u_s(x)$ and $\rho_s(x)$, in the top panel, and on the interfacial plane, $u_s(y)$, in the lower panel, in the presence and absence of pre-existing misfit dislocation, respectively.

3.5. *Effect of pre-existing misfit dislocations*

Interfacial misfit dislocations, interacting with the applied stress, and incoming glide dislocations can be a potent barrier to slip transmission [15]. In this section we explore the effect of pre-existing misfit dislocations on the dislocation core properties and on the transmission stress. Two simulations are carried out in the absence and the presence of pre-existing misfit dislocation as follows:

- Initially, the interface has zero displacement content and there is only a single glide dislocation on the slip plane having a maximum displacement of 2.6 Å. After the dislocation transmits from Cu to Ni as shown in figure 6, it leaves part of its displacement on the interface. Therefore, the original displacement on the glide plane is reduced from 2.6 Å to 2.35 Å, whereas that on the interface is increased from 0 to 0.25 Å.
- Initially, we consider both a glide and pre-existing misfit dislocation on the slip and the interfacial planes, respectively. The maximum displacement contents on both the interfacial and glide plane are equal (2.6 Å). The fractional dislocations on the interface are allowed to interact with the glide fractional dislocations, where the glide fractional dislocations are allowed to spread on the interfacial plane and vice versa. After the dislocation transmission as shown in figure 6, the displacement content on the glide and interfacial planes

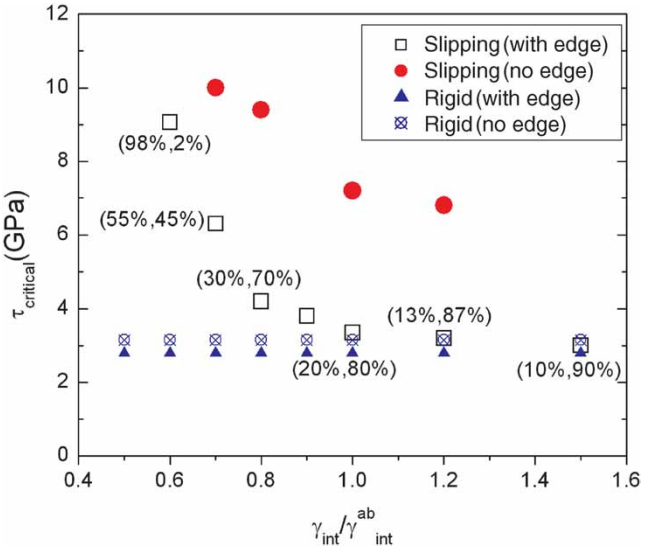

Figure 8. The variation of the critical shear stress with the GSFS of the interface. Rigid interface does not accommodate core spreading and therefore it is not affected by the change in interfacial GSFS. The removal of the edge component leads to a significant increase in the transmission stress for the slipping interface case and minor increase for the rigid interface case.

do not change from their initial values, indicating that the presence of a pre-existing dislocation prevents any spreading from or to the glide plane.

The screw displacement and density profiles on the glide plane, $u_s(x)$ and $\rho_s(x)$, and on the interfacial plane, $u_s(y)$ after the glide dislocation has been transmitted are shown in figure 7, in the absence (dotted curves) and the presence (solid curves) of the misfit interfacial dislocation. The results indicate that the transmission stress increases dramatically compared to its corresponding value in the absence of the misfit dislocation. Note, that there is no ledge formation on the interface when the misfit dislocation is present.

Figure 8 shows the critical transmission stress versus the ratio of γ_{int} with respect to its a*b initio* value for the cases of a non-slipping (rigid) and a slipping interface, with and without the edge component taken into account. The number in parenthesis indicates the percentage dislocation content on the interface for the case of slipping interface with the edge component taken into account. As expected, the critical transmission stress is independent of γ_{int} for the case of a rigid interface, and its value is higher when the edge component is neglected in the simulations. For the case of a slipping interface, i.e. when $\gamma_{int} < \gamma^{ab}_{int}$, the interface allows more dislocation content to spread from the glide plane to the interface. This in turn leads to a dramatic increase in the critical stress for transmission. For example, the critical stress is increased by a factor of three for $\gamma_{int} = 0.60\gamma^{ab}_{int}$, compared to the corresponding value at $\gamma_{int} = \gamma^{ab}_{int}$. On the other hand, when $\gamma_{int} > \gamma^{ab}_{int}$, the GSFS of the interface increases, the interfacial slipping becomes more difficult and the critical stress

decreases more slowly saturating to a value of about 2.8 GPa. Thus, these results clearly demonstrate that the increase of transmission stress is directly related to the spreading process on the interface. Note that the percentage of dislocation content on the interface increases from about 10% at $\gamma_{\text{int}} = 1.50\gamma_{\text{int}}^{ab}$ to 98% at $\gamma_{\text{int}} = 0.60\gamma_{\text{int}}^{ab}$. A similar trend of the critical transmission stress as a function of the interfacial energy barrier is also found for the case of slipping interface without taking into account the edge components (plain circles), but with higher values of critical stress. Our calculations show for the first time that the removal of the edge components results in dramatically different values for the transmission stress compared to those if the dissociation is included.

4. Conclusions

We have presented a hybrid approach to study the dislocation transmission/spreading in both coherent and semi-coherent Cu/Ni bimaterial. This approach combines the parametric dislocation dynamics based of the PN framework with *ab initio*-determined GSFS. The model takes into account all three components of atomic displacements of the dislocation and utilizes the entire GSFS to reveal outstanding features of dislocation dissociation. The effects of the mismatch in the elastic properties, gamma surfaces, and misfit dislocations on the spreading of the dislocation at the interface and on the transmission across the interface are accounted for. We are able to reproduce several MD simulations trends and make further predictions about the strength of Cu/Ni laminates, without the reliance on empirical potentials. Our calculations show that the dislocation dissociates into partials in both Cu and Ni. The dislocation core is squeezed near the interface facilitating the spreading process, and leaving an interfacial ledge during the transmission process. The dependence of the critical transmission stress on the dislocation spreading/transmission is examined. The competition of dislocation spreading and transmission depends on the GSFS of the interface. It is found that the decrease of the interfacial GSFS enhances core spreading which in turn increases the transmission stress. Moreover, it is found that the strength the bimaterial can be significantly enhanced by the presence of pre-existing misfit dislocations. In contrast to other available PN models, it is shown that dislocation core spreading in the two dissimilar materials and on their common interface must be simultaneously considered because of the significant effects on the transmission stress.

Acknowledgements

The authors are very grateful to R. Hoagland for his helpful comments. This research was performed under the auspices of the United States Air force Office of Scientific Research (AFOSR) grant number F49620-03-1-0031 and the US Army Research Office (ARO) under grant No. W911NF-04-1-0058. G. Lu acknowledges the support from the ACS Petroleum Research Fund.

References

[1] A. Misra, J.P. Hirth and H. Kung, Phil. Mag. A **82** 2935 (2002).
[2] A. Misra and H. Kung, Adv. Engng. Mater. **3** 217 (2001).
[3] B.M. Clemens, K. Kumg and S.A. Barnett, MRS Bull. **24** 20 (1999).
[4] L. Fang and L.H. Friedman, Phil. Mag. **85** 3321 (2005).
[5] E.O. Hall, Proc. Phys. Soc. B **64** 747 (1952).
[6] N.J. Petch, J. Iron Steel Inst. **174** 25 (1953).
[7] P.M. Anderson and C. Li., Nanostruct. Mater. **5** 349 (1995).
[8] J.S. Koehler, Phys Rev. B **2** 54 (1970).
[9] T. Foecke and D. vanHeerden, in *Chemistry and Physics of Nanostructures and related Non-equilibrium Materials*, edited by E. Ma, B. Fultz, R. Shull, *et al.* (TMS, Pittsburgh, PA, 1997).
[10] P.M. Anderson, T. Foecke and P.M. Hazzledine, MRS Bull. **24** 27 (1999).
[11] L.E. Shilkrot and D.J. Srolovitz, Acta Mater. **46** 3063 (1998).
[12] X. Han and N.M. Ghoniem, Phil. Mag. **85** 1205 (2005).
[13] A.K. Head, Proc. Phys. Soc. LXVI **9B** 793 (1952).
[14] A.K. Head, Phil. Mag. **7** 44 (1953).
[15] R.G. Hoagland, T.E. Mitchell, J.P. Hirth, *et al.*, Phil. Mag. **82** 643 (2002).
[16] I. Rao and P.M. Hazzledine, Phil. Mag. A **80** 2011 (2000).
[17] A. Misra, J.P. Hirth and R.G. Hoagland, Acta Mater. **53** 4817 (2005).
[18] G. Schoeck, Acta Mater. **49** 1179 (2001).
[19] G. Schoeck, Mater. Sci. Engng A **333** 390 (2002).
[20] G. Lu, N. Kioussis, V. Bulatov, *et al.*, Phys. Rev. B **62** 3099 (2000).
[21] G. Lu, V. Bulatov and N. Kioussis, Phys. Rev. B **66** 144103 (2002).
[22] G. Lu, Q. Zhang, N. Kioussis, *et al.*, Phys. Rev. Lett. **87** 95001 (2001).
[23] R. Miller, R. Phillips, G. Beltz, *et al.*, J. Mech. Phys. Solids **46** 1845 (1998).
[24] P.M. Anderson and Z. Li, Mater. Sci. Engng A **319** 182 (2001).
[25] Y. Shen and P.M. Anderson, TMS Lett. **1** 17 (2004).
[26] Y. Shen and P.M. Anderson, Acta Mater. **54** 3941 (2006).
[27] N.M. Ghoniem, S.H. Tong and L.Z. Sun, Phys. Rev. B **61** 913 (2000).
[28] S. Banerjee, N.M. Ghoniem, N. Kioussis, paper presented at the Second International Conference on Multiscale Materials Modelling, Los Angeles, 11–15 October (2004).
[29] C.H. Henager Jr and R.G. Hoagland, Scripta Mater. **50** 701 (2004).
[30] G. Kresse and J. Joubert, Phys. Rev. B **59** 1758 (1999).
[31] G. Kresse and J. Hafner, Phys. Rev. B **47** 588 (1993).
[32] G. Kresse and J. Furthmuller, Phys. Rev. B **54** 11169 (1996).
[33] N. Bernstein and E.B. Tadmor, Phys.Rev. B **69** 094116 (2004).